*Science & Technology Development Journal – Engineering and Technology 2024, 6(SI7):69-85*

Open Access Full Text Article

**Research Article**

# Geochemical and petrological properties of the Neogene shale gas in the central Song Hong basin, Vietnam

Vo Thi Hai Quan[1,*], Pham Huy Giao[1,2], Anna Wysocka[3]

**ABSTRACT**

Song Hong basin or the Red River basin is generally considered to be composed up of three units, and namely, the northern, central and southern parts, among which the central Song Hong basin has been much less explored comparing to the other units. The recent discovery of gas in this part of Song Hong basin has raised the interests of the local and overseas explorationists studying and assessing to better understanding of hydrocarbon generation potential of source rocks in this area. In this study, the Pliocene and Upper Miocene shale samples, which taken from A-1X well in the central Song Hong basin, are analyzed for the source rock characteristics and petroleum generation potential based on geochemical, well log, X-Ray Diffraction data and 1D petroleum system modeling. It was found that the total organic carbon contents are poor for the Pliocene shales and poor to fair for the Upper Miocene shales ranging from 0.15-0.21 wt.% and 0.19-0.79 wt.%, respectively, indicating poor to fair source rock generation potential for both shales. The organic matters are mainly derived from higher plants of type III kerogen and possibly mixing a minor amount of type II kerogen from algae. Vitrinite reflectance values range from 0.45-0.65% for Pliocene and 0.72-0.93% for part of Upper Miocene shales, showing a good match with bottom hole temperature of 163$^o$C. The burial and thermal history models indicate that the rapid sedimentation rate affected the increase in temperature in the Pliocene and Upper Miocene shales as mature source rocks and reached peak of oil generation. The models show the early hydrocarbon generation (Ro=0.60 %) in the Pliocene and the main phase of hydrocarbon generation (Ro=0.80 %) in the Upper Miocene. As results of this study, Pliocene and Upper Miocene shales can be considered having a potential to generate gas from both biogenic and thermogenic origins. It was estimated that the gas generation is about 17.88 Mtons, the gas expulsion approximately 4.3 Mtons/km$^2$ and the remaining of kerogen of about 62.81 Mtons, gas initial in place of about 1.49 (Tcf). It is thought that the deeper shales are more effective source rocks, which need to be drilled more for new gas prospects.

**Key words:** Shale gas, Source rock, Vitrinite reflectance, XRD, Petroleum system, Song Hong Basin

[1]*Geochemical laboratory, Vietnam Petroleum Institute, Vietnam*

[2]*Lecturer, PetroVietnam University; Expert, Vietnam Petroleum Institute, Vietnam*

[3]*Faculty of Geology, University of Warsaw, Poland*

**Correspondence**

**Vo Thi Hai Quan**, Geochemical laboratory, Vietnam Petroleum Institute, Vietnam

Email: quanvth@vpi.pvn.vn

**History**

- Received: 29-9-2023
- Accepted: 17-5-2024
- Published Online: 31-12-2024

**DOI : 10.32508/stdjet.v6iSI7.1238**

Check for updates

**Copyright**

© VNUHCM Press. This is an open-access article distributed under the terms of the Creative Commons Attribution 4.0 International license.

## INTRODUCTION

The Song Hong Basin (SHB) or the Red River Basin is a pull-apart basin with different local geological properties that divided into three structural units, and namely, the northern, central and southern parts (Figure 1). So far the hydrocarbon exploration and production activities carried out by the PetroVietnam and oil companies have been mainly done in the northern and southern parts of the basin [1].

Although the central SHB is less explored some recent discoveries have awaken great interests to study better the petroleum system in this part of SHB. In this study the A-1X well is selected. The well's final depth was 3,603 m reaching the Upper Miocene. The elements of petroleum system such as source rocks, seals, and reservoirs were defined. 1D petroleum system modeling was conducted to estimate timing of hydrocarbon generation and migration into reservoirs.

## GEOLOGICAL SETTING

The central SHB spreads from blocks 105 to 114, where the sedimentary deposits were supposed quite stable and not much affected by tectonic activity. Sediments in the depocenter part are mostly fine-grained stratigraphically a top Upper Miocene-Pliocene shale diapirs [2] and [3]. The Pliocene sediments had undergone tectonic uplift and inversion in the NW of the Gulf of Bac Bo to form the uplifted Dong Son. Due to the sediment influx, sand bodies in Upper Miocene-Lower Pliocene were usually deposited in submarine fans and turbidity facies, spreading from the NW to the SE (Figure 3). Significant prospects include low magnitude four-way dip closures on the Dong Son uplift and four-way dip closures developed on the shale diapirs [1], i.e., the Dong Fang and Le Dong gas wells in China or turbidities/submarine fans to the East of central blocks.

VNUHCM PRESS

**Cite this article :** Quan V T H, Giao P H, Wysocka A. **Geochemical and petrological properties of the Neogene shale gas in the central Song Hong basin, Vietnam**. *Sci. Tech. Dev. J. – Engineering and Technology* 2024; 6(SI7):69-85.

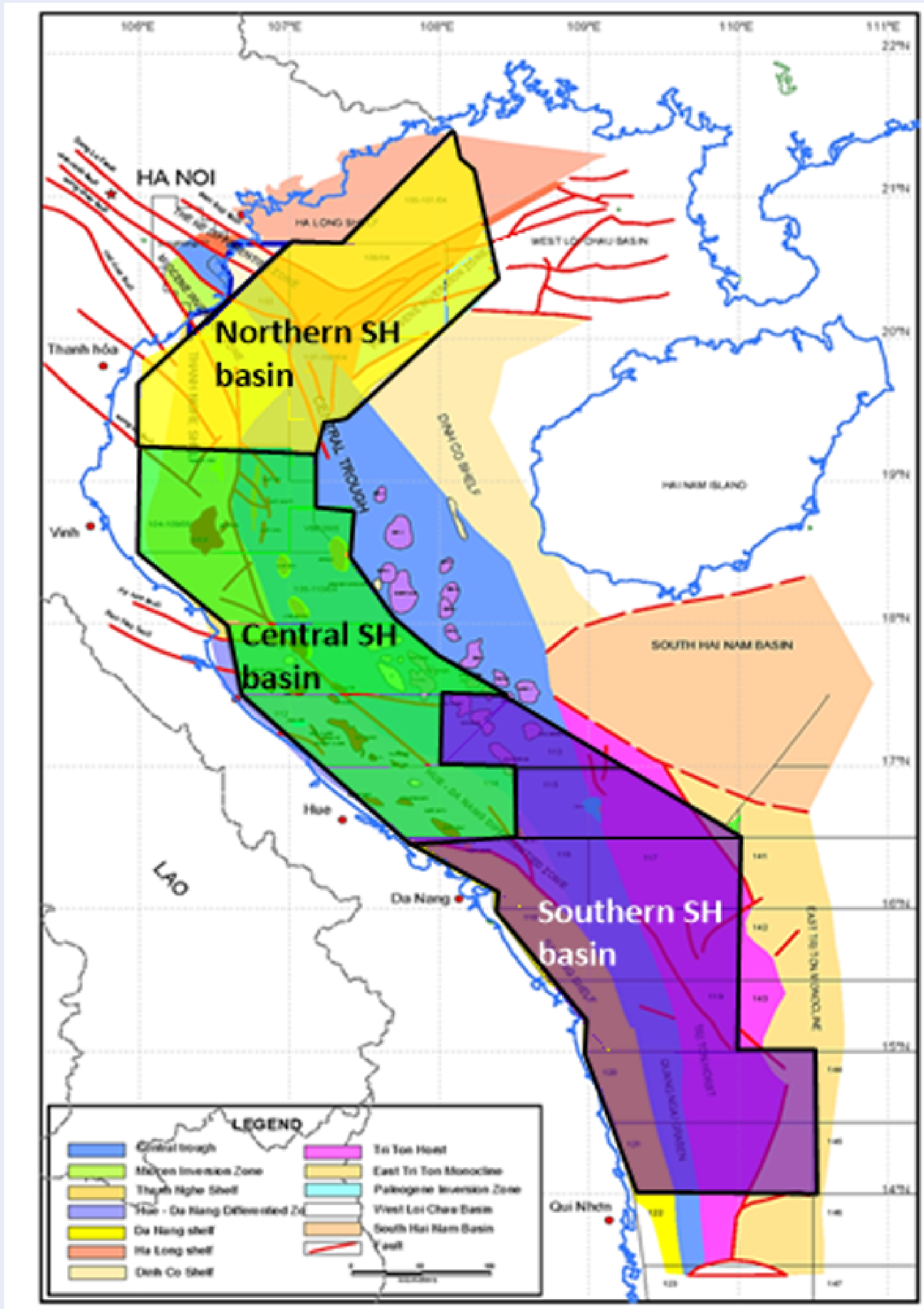


**Figure 1**: Main structural elements of the central Song Hong basin [1]

Alongside the coast of central part of the SHB, the basement is predominantly consist of Upper Ordovician-Silurian carbonates, gritstone/conglomerates, sandstones, and schist of the Long Dai and Song Ca Formations (Fm), Lower Devonian sandstones and conglomerates of the Tan Lam Fm, Middle-Upper Devonian carbonates of the Cu Bai Fm, and other granite-biotite intrusive, etc. (Figure 3). These formations tend to develop seawards, and have possibly being formed the buried traps that later turned into important hydrocarbon reservoirs as discovered in the Bach Tri and Hai Yen structures [1].

The Hue-Da Nang shelf is restricted by the onshore Song Ca and Rao Nay fault systems. This area was dominated with left lateral strike-slip fault systems, forming a whole series of echelon blocks of horst and graben structures at the end of Oligocene (Figure 2). The most important geological structures in this region are the Anh Vu-Da Nang graben and Hai Yen-Bach Tri-Than Nong high with uplifted prior to the Lower Oligocene and syn-sedimentation continuing in the Lower Miocene. Upper Oligocene-Lower Miocene inversion occurred in some grabens or half-grabens, i.e. prospects in blocks 111 and 114. Middle-Upper Devonian carbonate drapes developed on top of the basement highs, i.e. Hai Yen and Bach Tri prospects, four-way dip closures formed in the Miocene clastics, i.e. the Dai Bang prospect; Oligocene-Lower Miocene inversion and minor reef build-up are important exploration targets in this region [1].

In the central SHB, lots of gas accumulations were discovered in the Miocene carbonate build-up and in the Tri Ton uplift, i.e., 115-A-1X, 118-CVX-1X, 119-CH-1X. The gas is very rich in $CO_2$ content that probably caused by the high geothermal temperature or thermal convection from the mantle in this area [1].

## DATA AND METHODS

### Sample collection

Thirty-six cutting samples from were used for geochemical and petrology analyses such as Rock-Eval pyrolysis, vitrinite reflectance and XRD. In addition, well log curves taken from VPI are used for lithological reference. Geochemical results are used to evaluate source rock characteristics and also for 1D petroleum system modeling and volumetric calculations.

### Analytical methods

#### Rock-Eval pyrolysis (RE)

Parameters from Rock-Eval 6 pyrolysis, i.e., TOC, S1, S2, HI, PI, Tmax are used for characterization of the quantity, quality, and level of thermal maturity of organic matters for the source rocks in any sedimentary basin (Tables 1 and 2). This analysis was performed at VPI-Labs. The results are presented at Table 3.

Basically, the RE is conducted on rock sample, typically about 50-100 mg, which was placed into a crucible that will be moved into the pyrolytic oven. The rock samples are heated in the inert gas of Helium (He) at 300$^o$C and kept isothermal condition up to five minutes. During the time, the evaporative organic materials are recorded by a Flame Ionization Detector (FID) and named as $S_1$ peak. Continuing the isothermal heating, rock samples are still kept in the linearly increasing thermal condition from 300 to 650$^o$C at the rate of 25$^o$C per minute, and the $S_2$ peak was recorded. The temperature Tmax ($^o$C) is defined at peak $S_2$ and used as the thermal maturity parameter. An infrared cells (IR) detects amount of $CO_2$ (mg$CO_2$/g original rock) named as $S_3$ peak. This $CO_2$ content is generated during the progress of isothermal heating steps and setting up to 400$^o$C. $CO_2$ which released between 400 and 650$^o$C is measured by the decomposion of carbonate minerals through heating. Pyrolysis mineral carbon or type of kerogen is determined based on CO and $CO_2$ produced during pyrolysis and oxidation state. Total organic carbon (TOC, wt. %) is calculated from the quantity of the pyrolysis organic carbon [4].

#### Vitrinite Reflectance

Kerogen, which is isolated from organic matters of shale samples, is blocked in epoxy resin. The block is polished and then measured under CRAIC 308$^{TM}$ spectrometry microscope with oil immersion and performed at VPI-Labs. Good vitrinite particles are selected for measurement in a random mode. Depending on number of particles presenting in the sample, about 50 measurement readings are enough for getting final reliable value (Ro, %).

#### X-Ray Diffraction

A standard XRD analysis for whole rock and shale is performed at VPI-Labs to define quantitative and qualitative mineral compositions which are needed for determination of the brittleness shale. The XRD analysis is carried out on the D8-Advance automatic system with alternative system 40 (kV) and 40 (mA), using Copper K-a radiation with Nickel filter, step width of 0.04$^o$ and counting time 1 second per step.

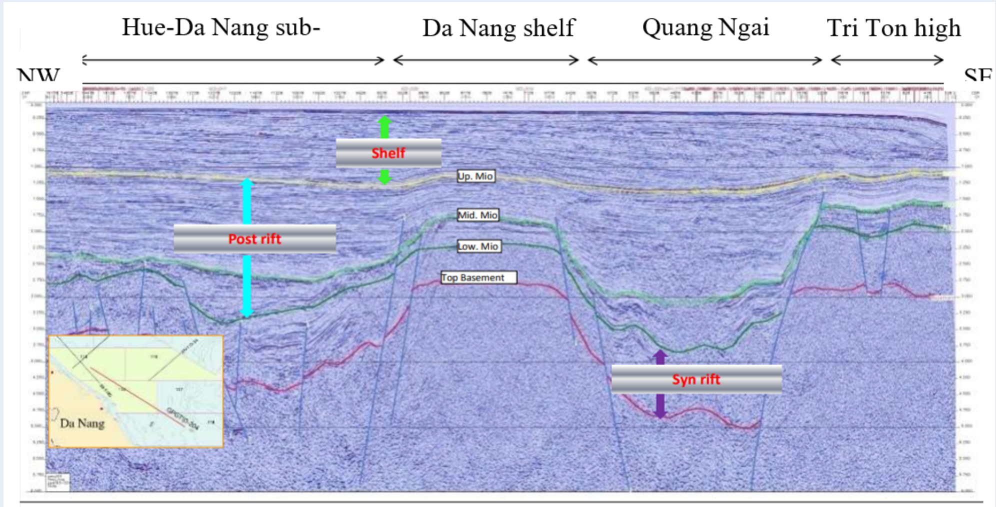


**Figure 2**: Seismic section through some blocks in the central SHB [1]

**Table 1: Guideline for source rock interpretation [5]**

| Quantity | TOC | S1<br>(mg HC/g rock) | S2<br>(mg HC/g rock) |
|---|---|---|---|
| Poor | <0.5 | <0.5 | <2.5 |
| Fair | 0.5-1.0 | 0.5-1 | 2.5-5 |
| Good | 1-2 | 1-2 | 5-10 |
| Very good | 2-4 | 2-4 | 10-20 |
| Excellent | >4 | >4 | >20 |
| Quality | | (mg HC/g TOC)<br>HI | Kerogen type |
| Non hydrocarbon | | <50 | IV |
| Gas | | 50-200 | III |
| Gas and oil | | 200-300 | II/III |
| Oil | | 300-600 | II |
| Oil | | >600 | I |

**Table 2: Parameters of source rock maturity [6]**

| Level of maturation | Ro (%) | Tmax (oC) | PI |
|---|---|---|---|
| Immature | 0.2-0.55 | <435 | <0.10 |
| Marginal mature | 0.55-0.60 | - | - |
| Mature<br>Early mature | 0.60-0.65 | 435-445 | 0.10-0.25 |
| Peak mature | 0.65-0.90 | 445-450 | 0.25-0.40 |
| Late mature | 0.90-1.35 | 450-470 | >0.40 |
| Post mature | >1.35 | >470 | - |

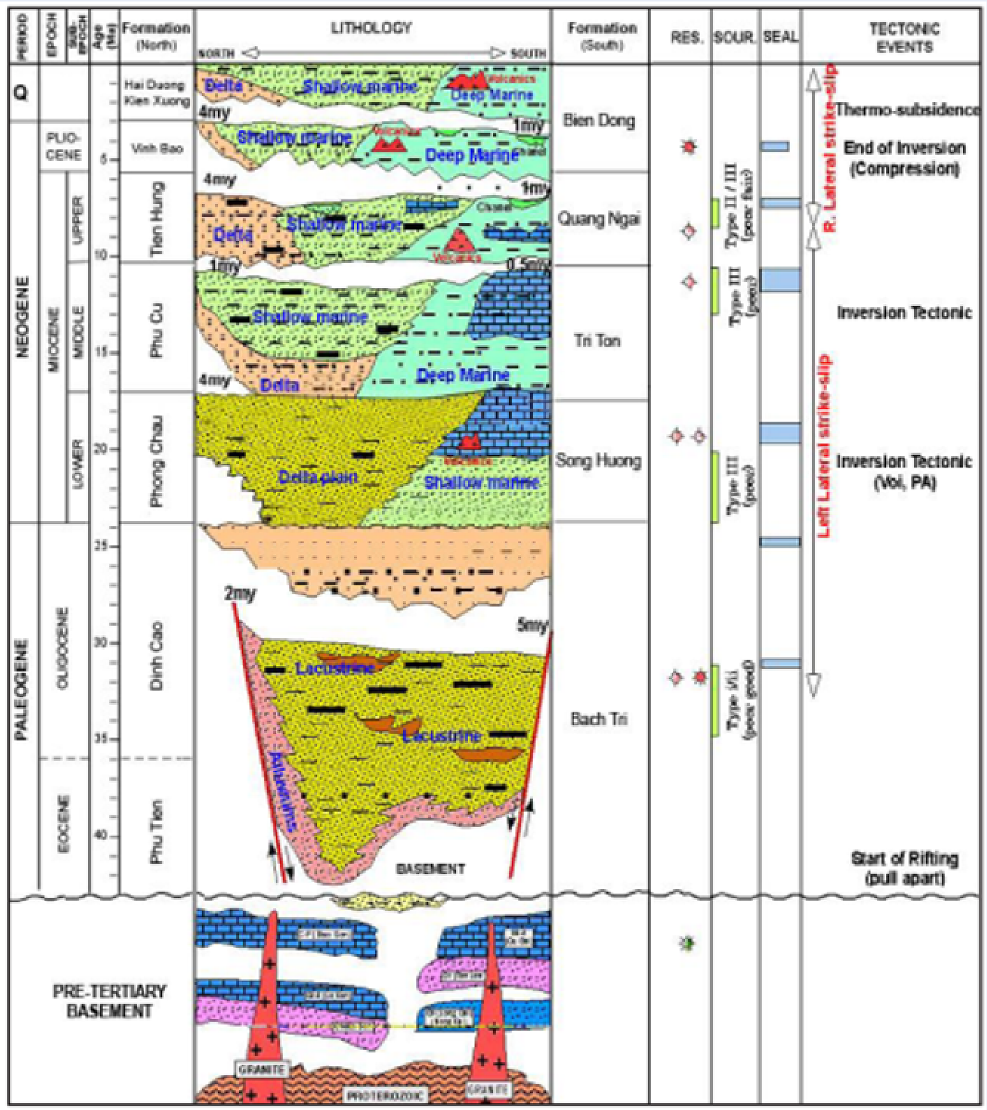

**Figure 3**: Stratigraphic column from the North to the South of SHB [1]

Whole rock analysis is carried out using approximately 1g of sample that is ground by micronizing mill; powder sample is then packed to plastic sample holder and run from $3^o$2q-$50^o$2q. The XRD analysis for clay fraction runs from $2^o$2q to $30^o$2q including four traces are done following steps: (i) drying the clay mount at room temperature and humidity; (ii) ethylene glycol solvation for 24 hours at $50^o$-$60^o$C in order to identify swelling clays in sample; (iii) immediately following heat to $300^o$C for 30 minutes. This causes illite-smectite and smectite to concur at 10 (Å); (iv) heat to $550^o$C for 1.5 hours, causing the destruction of brucite and kaolinite minerals within chlorite [7].

### 1D petroleum system modeling

Basin modeling is a useful method for reconstructing the burial and thermal evolutions of a sedimentary basin. In this study, the A-1X well was selected for 1D petroleum system using PetroMod 11 software (Schlumberger). The input data include the depths, age, lithologies, sediment thickness, erosion thickness, kerogen types and kinetics (Table 6). These input data were derived from well log data, biostratigraphy, local geology, geochemical parameters. The models are constructed depending upon considering three scenarios of boundary conditions, i.e., sediment water interface temperature (SWIT), paleowater depth (PWD), and the present-day heat flow

and paleo-heat flow (HF)[8].
SWIT is estimated by Wygrala (1989)'s equation[9], varying in the mean surface paleo temperatures versus northern Southeast Asia latitude and geological time. PWD values are needed for calculating the SWIT. The PWD values are defined from inner shelf to shallow marine environments by combination of tectonic subsidence and global sea level changes. High geothermal gradient is calculated from borehole temperature based on PVN (2019)[1]. The crustal stretching model of Mckenzie (1978)[10] is used to calculate the heat flow variation through time. Paleo-heat flow estimation is constrained by present-day heat flow and calibrated from vitrinite reflectance, bottom hole temperature and tectonic events. The easy %Ro kinetic model of Sweeney and Burnham (1990)[11] is applied for calculating levels of thermal maturity. Burnham_$CO_2$_TIII[12] is the main kinetic model that is used for calculating petroleum generation in this paper. Other kinetics such as Burnham (1989)_TIII and Pepper & Corvi (1995)_TIII(H) DE[13] are used for comparison with the main kinetic model. The main outputs obtained from the simulation, i.e., burial and thermal histories, thermal conductivity, porosity, transformation ratio, etc. are further used for characterizing petroleum system at this well location and estimating the gas initial in place (GIIP) as follows:

GIIP = (43,560*A*h*$\phi$*Sg) /Bg [MMScf]

Where: A = area (acre) is estimated from area of studied blocks

h = net thickness (ft.) of rich shale zone

j = porosity (fraction)

Sg = the fraction of the porosity filled by gas (fraction)

Bg = formation volume factor of gas ($ft^3$/scf)

z = compressibility factor of gas, Bg = 0.028zT/P

# RESULTS AND DISCUSSION

## Source rock properties

### Organic matter richness and source rock quality

Rock-Eval pyrolysis parameters are used for quantitative and qualitative assessments of organic matters of thirty-five shale samples in Pliocene and Upper Miocene formations. Pliocene shales, from 1510 to 2645 m depth, were found to be poor in organic richness and hydrocarbon generation potential, i.e., they are of type III kerogen with TOC ranging from 0.13 to 0.21 wt.%, pyrolysis yields (S1+S2) varying from 0.20 to 0.40 mgHC/g rock and HI ranging from 103 to 196 mgHC/g TOC, respectively. These indicate that the Pliocene shales are not potential source rocks. The Upper Miocene shales from 2,700 to 3,603 m show low total organic carbons and hydrocarbon generation potential of type III kerogen with TOC varying between 0.19 to 0.24 wt.%, (S1+S2) yields ranging from 0.50 to 0.62 mgHC/g rock, HI varying between 155 and 199 mgHC/g TOC, respectively. On the other hand, the Upper Miocene shales in the 3005-3603 m interval display moderate total organic carbon contents and pyrolysis yields with TOC varying between 0.56 and 0.79 wt.%, (S1+S2) ranging from 0.85 to 2.51 mgHC/g rock, respectively. The organic matters are originated from kerogens of type III and mixing type III/II with HI ranging from 109 to 296 mgHC/g TOC. Consequently, the Upper Miocene shales are poor to fair potential source rocks that mainly generate gas (Table 3; Figures 4, 5 and 6).

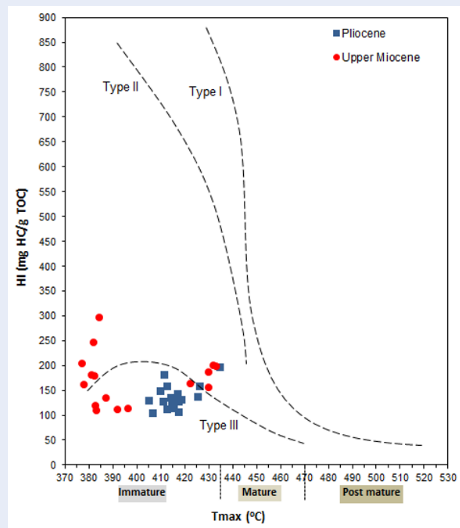


**Figure 5**: Types of organic matters

### Thermal maturity

PI and Tmax values are used as maturity indicators together with vitrinite reflectance ($R_0$). Organic matters of shales in the Pliocene are in immature to early mature stage with PI, $T_{max}$ and Ro ranging from 0.13 to 0.22, 405 to 435$^oC$, and 0.45 to 0.65 %, respectively. Organic matters have entered the early mature stage at 1,850 m in Pliocene and reached the peak of maturity in Upper Miocene starting at 2,760 m through 3290 m, corresponding to PI of 0.31 and Ro of 0.72 %. Organic matters of the Upper Miocene shales in the interval from 3,345 to 3,603 m show an immature stage with Ro ranging from 0.40 to 0.50 %. However, in the Upper Miocene, Tmax values are not consistent with PI and vitrinite reflectance values in the

**Table 3: Rock-Eval pyrolysis and vitrinite reflectance**

| Depth (m) | | | TOC | S1 | S2 | S3 | HI | PI | Tmax | Ro |
|---|---|---|---|---|---|---|---|---|---|---|
| | | | (wt.%) | (mgHC/g rock) | | | (mgHC/g | | ($^{o}$C) | (%) |
| Pliocene | | | | | | | | | | |
| 1510 | - | 1530 | 0.21 | 0.06 | 0.22 | 1.14 | 103 | 0.21 | 407 | 0.45 |
| 1610 | - | 1630 | 0.21 | 0.04 | 0.27 | 1.47 | 128 | 0.13 | 416 | 0.46 |
| 1670 | - | 1690 | 0.16 | 0.04 | 0.20 | 1.53 | 128 | 0.17 | 405 | 0.51 |
| 1730 | - | 1750 | 0.15 | 0.03 | 0.17 | 1.60 | 110 | 0.15 | 413 | 0.53 |
| 1790 | - | 1810 | 0.13 | 0.04 | 0.23 | 0.96 | 180 | 0.15 | 412 | 0.52 |
| 1850 | - | 1870 | 0.15 | 0.04 | 0.23 | 1.15 | 156 | 0.15 | 413 | 0.58 |
| 1910 | - | 1930 | 0.16 | 0.03 | 0.21 | 1.20 | 134 | 0.13 | 415 | 0.59 |
| 1970 | - | 1990 | 0.18 | 0.05 | 0.22 | 1.57 | 123 | 0.19 | 415 | 0.58 |
| 2030 | - | 2050 | 0.19 | 0.04 | 0.20 | 1.65 | 106 | 0.17 | 418 | 0.59 |
| 2090 | - | 2110 | 0.18 | 0.06 | 0.23 | 1.60 | 126 | 0.21 | 411 | 0.55 |
| 2170 | - | 2190 | 0.19 | 0.05 | 0.24 | 1.72 | 126 | 0.17 | 418 | 0.61 |
| 2230 | - | 2250 | 0.16 | 0.06 | 0.22 | 1.62 | 141 | 0.21 | 417 | 0.59 |
| 2290 | - | 2310 | 0.16 | 0.06 | 0.21 | 1.45 | 134 | 0.22 | 415 | 0.62 |
| 2350 | - | 2370 | 0.17 | 0.06 | 0.22 | 1.52 | 129 | 0.21 | 419 | 0.60 |
| 2410 | - | 2430 | 0.16 | 0.05 | 0.24 | 1.67 | 148 | 0.17 | 410 | 0.61 |
| 2450 | - | 2470 | 0.20 | 0.04 | 0.22 | 1.21 | 113 | 0.15 | 416 | 0.50 |
| 2530 | - | 2540 | 0.21 | 0.06 | 0.29 | 1.71 | 136 | 0.17 | 426 | 0.60 |
| 2580 | - | 2590 | 0.20 | 0.08 | 0.31 | 1.62 | 157 | 0.21 | 427 | 0.65 |
| 2640 | - | 2650 | 0.16 | 0.06 | 0.32 | 1.12 | 196 | 0.16 | 435 | - |
| Upper Miocene | | | | | | | | | | |
| 2700 | - | 2710 | 0.24 | 0.11 | 0.37 | 1.43 | 155 | 0.23 | 430 | - |
| 2760 | - | 2770 | 0.23 | 0.19 | 0.43 | 1.52 | 186 | 0.31 | 430 | 0.72 |
| 2820 | - | 2830 | 0.21 | 0.12 | 0.42 | 1.39 | 199 | 0.22 | 432 | 0.77 |
| 2880 | - | 2890 | 0.19 | 0.11 | 0.37 | 1.30 | 197 | 0.23 | 433 | 0.76 |
| 2940 | - | 2945 | 0.23 | 0.14 | 0.37 | 1.41 | 162 | 0.27 | 422 | 0.73 |
| 3005 | - | 3010 | 0.56 | 0.18 | 0.90 | 1.45 | 161 | 0.17 | 378 | 0.82 |
| 3060 | - | 3065 | 0.69 | 0.18 | 0.82 | 1.65 | 118 | 0.18 | 383 | 0.69 |
| 3120 | - | 3125 | 0.69 | 0.23 | 2.05 | 1.58 | 296 | 0.10 | 385 | 0.70 |
| 3180 | - | 3185 | 0.69 | 0.21 | 1.23 | 1.80 | 179 | 0.15 | 382 | 0.85 |
| 3230 | - | 3235 | 0.76 | 0.20 | 1.37 | 1.73 | 180 | 0.13 | 381 | 0.82 |
| 3285 | - | 3290 | 0.64 | 0.22 | 1.58 | 0.81 | 245 | 0.12 | 382 | 0.93 |
| 3345 | - | 3350 | 0.70 | 0.18 | 1.42 | 1.11 | 204 | 0.11 | 377 | 0.50 |
| 3405 | - | 3410 | 0.62 | 0.18 | 0.67 | 1.49 | 109 | 0.21 | 383 | 0.45 |
| 3470 | - | 3475 | 0.74 | 0.26 | 0.99 | 1.63 | 135 | 0.21 | 387 | 0.40 |
| 3530 | - | 3535 | 0.79 | 0.29 | 0.87 | 1.92 | 110 | 0.25 | 392 | 0.40 |
| 3595 | - | 3603 | 0.64 | 0.46 | 0.72 | 2.12 | 113 | 0.39 | 397 | 0.42 |

TOC=Total Organic Carbon; HI=S2/TOC; PI=S1/(S1+S2)

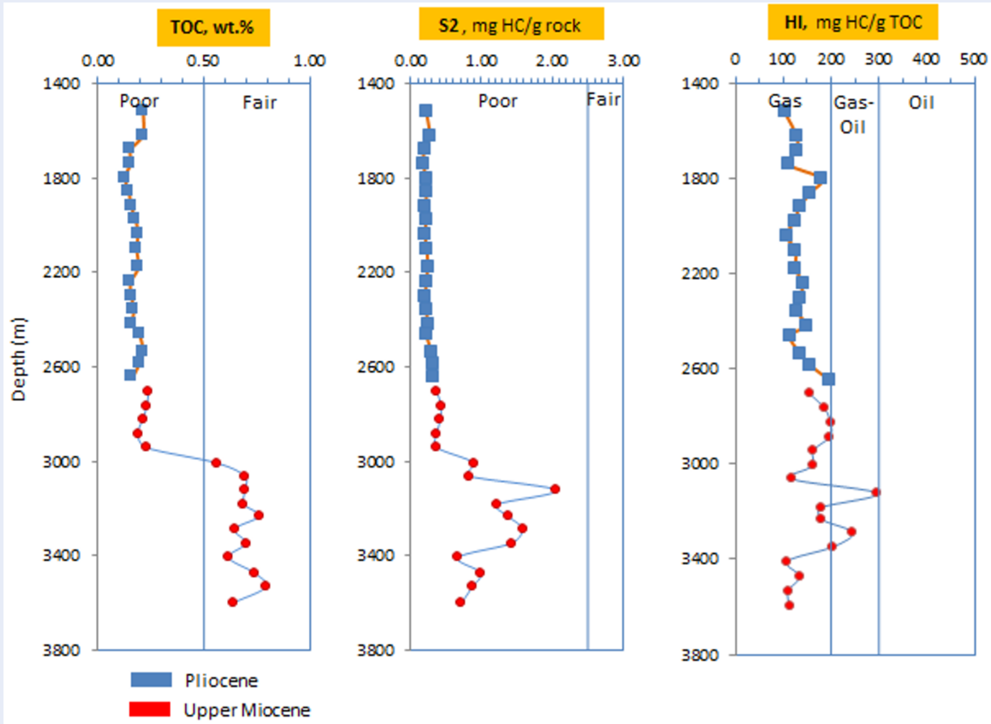


**Figure 4**: Change of Rock-Eval parameters with depth

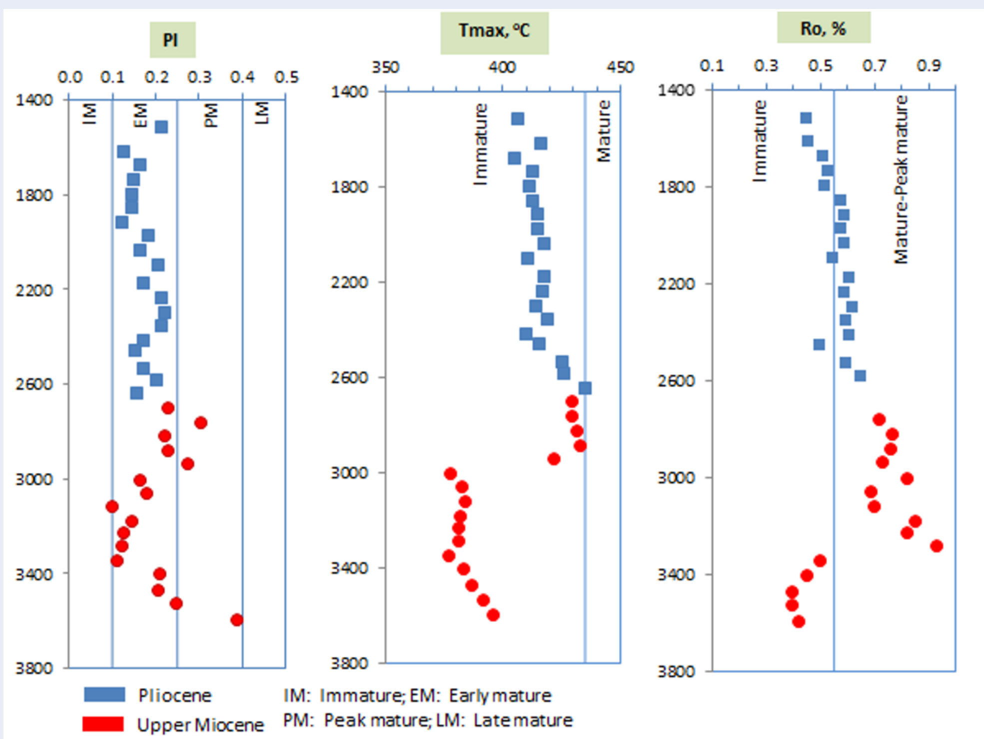


**Figure 7**: Change of parameters of thermal maturity with depth

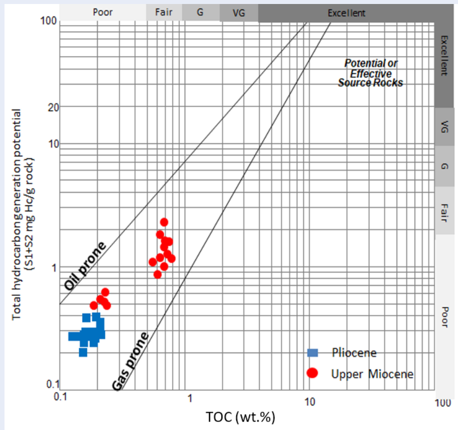


**Figure 6**: Total hydrocarbon generation and organic carbon

interval from 3,005 to 3,603 m, where the PI values ranging from 0.11 to 0.39 and the anomalous Tmax values of less than 400$^{o}$C suggest that these are possibly oil stains or the maturity threshold of the vitrinite particles is only reached at 3,290 m (Figure 7). Besides, the vitrinite profile shows the existence of a major thrust fault around 3,345 m, causing vitrinite reflectance values decreased or vitrinite reflectance values are anormalous in the interval 3,345-3,569m that may be a function of erosion [14].

## Mineral and clay compositions

Mineral assemblages of Upper Miocene sediments comprise the abundance of brittle minerals (68.8-88.4 %), i.e. quartz, barite, calcite, feldspar, plagioclase constituents (Table 4, Figure 8), followed by ductile minerals, i.e. illite, chlorite, kaolinite (10.6-28.5 %) (Table 5, Figure 9) and little contents of dolomite, siderite and rieberite (Table 4, Figure 10). The higher content of brittle minerals, the more easily complex fracture networks are established [15]. The clay mineral assemblages in the Upper Miocene sediments mainly contain Illite, chlorite and kaolinite. Illite content is the most abundant in clay minerals (known as illite-type) (Table 5), followed by chlorite and kaolinite contents. Moreover, the presence of calcareous minerals, i.e., calcite and dolomite in these shales indicate the sediments were deposited in eustatic sea level rise worldwide, and also related to terrigenous influxes, the syn- and post-depositional dissolution of dissolved planktonic organisms. Especially, the very high calcareous mineral of shales in the interval 2,985-3,150 m is related to the inner shelf with very high terrigenous influxes. The relative high kaolinite contents suggest a climatic warming trend during the Upper Miocene.

## 1D petroleum system modeling

### *Burial history*

Burial and thermal history models were constructed for the Upper Miocene to Pliocene formations with a total vertical depth of 3,603 m. Based on the regional tectonic activities of the SHB, a period of erosion occurred in Pliocene and Upper Miocene from 5.20-5.0 Ma with eroded thickness of about 12 m. Pliocene and Upper Miocene shales contain poor to moderate organic matters, mainly derived from type III kerogen and deposited in coastal plain/shallow marine. The burial history shows the main features of deposition comprising thick shales interbedded with very thin sands/silts that rapidly deposited in Pliocene (Figure 10A). The maximum and minimum drilled thicknesses of shale are 590 m (1,921-2,511 m) and 30 m (581-611 m), respectively in Pliocene (Figure 10A).

### *Thermal history and hydrocarbon generation*

The present-day thermal maturity is not affected by the rifting phase that has attained a maximum heat flow value of 75 mw/m2. The Upper Miocene formation was deposited as post-rift basin-fill sediments at shallow depth in Pliocene (Table 6). The shale intervals as well as the multiple organic-rich intervals of the Pliocene and Upper Miocene formations are relative low thermal conductivities. The geothermal gradient increases from the top to bottom. Moreover, the high sedimentation rate in Pliocene causes the decrease of temperature if the sedimentation rate is faster than the rate of thermal equilibrium [16].

The models were constructed based on the heat flow values from bottom of Upper Miocene to Pliocene varying from 67 to 75 mW/m$^2$ using McKenzie's model (1978). The heat flow values show a good fit between measured and calculated bottom-hole temperatures and vitrinite reflectivities (Figure 13). Organic matters of Pliocene shales show poor TOC contents and the shales entered early mature stage in the interval 1510-2223 m (Ro=0.55-0.70 %), reached the main stage of hydrocarbon generation in the interval 2223-2645 m (Ro=0.70-1.0 %). Thus, these shales are not effective source rocks for hydrocarbon generation. Organic matters in Upper Miocene shales contain poor to fair TOC contents and reached peak hydrocarbon generation in the interval 2700-2986 m (Figure 10B). The shales entered wet gas/condensate phase in the interval 2,986-3,456 m, and dry gas phase below 3,456

**Table 4: Mineral compositions of Upper Miocene sediments**

| Depth (m) | Quartz | K-Feldspar | Plagio-clase | Clay min-erals | Calcite | Dolomit | Siderite | Pyrite | Riebe-cite | Zeolite | Barite |
|---|---|---|---|---|---|---|---|---|---|---|---|
| 2905-2920 | 70,7 | 5,4 | 3,3 | 11,60 | 2,1 | 2,2 | 0 | 0 | 0 | 0 | 4,7 |
| 2920-2930 | 47,2 | 3,8 | 2,6 | 21,9 | 2,9 | 0 | 4,3 | 4 | 0 | 0 | 13,3 |
| 2985-2995 | 18,8 | 2 | 2,1 | 11,0 | 49,4 | 3,4 | 3,6 | 2,5 | 0 | 0 | 7,2 |
| 2995-3005 | 17,5 | 2,2 | 1,8 | 11,2 | 51,8 | 3,3 | 2,8 | 0,0 | 1,7 | 4 | 3,7 |
| 3020-3030 | 25,0 | 7,4 | 2,1 | 15,3 | 26,6 | 6,5 | 0,0 | 0,0 | 0 | 0 | 17,1 |
| 3140-3150 | 18,1 | 4,0 | 1,9 | 19,4 | 24,8 | 4,2 | 0,0 | 0,0 | 3,7 | 8,1 | 15,8 |
| 3150-3160 | 54,5 | 3,7 | 8,4 | 13,5 | 2,8 | 12,0 | 0,0 | 0,0 | 0 | 0 | 5,1 |
| 3165-3175 | 49,4 | 4,0 | 2,6 | 16,9 | 9,0 | 5,2 | 0,0 | 3,6 | 0 | 0 | 9,3 |
| 3310-3320 | 54,9 | 4,4 | 3,5 | 16,2 | 3,4 | 4,1 | 0,0 | 3,1 | 0 | 0 | 10,4 |
| 3320-3330 | 64,2 | 3,3 | 12,6 | 10,6 | 4,3 | 0,0 | 0,0 | 0,0 | 0 | 0 | 5,0 |
| 3405-3415 | 64,7 | 3,7 | 4,5 | 14,7 | 4,1 | 5,0 | 0,0 | 0,0 | 0 | 0 | 3,3 |
| 3415-3425 | 59,2 | 5,5 | 3,8 | 13,1 | 3,5 | 4,2 | 0,0 | 0,0 | 0 | 0 | 10,7 |
| 3425-3435 | 56,1 | 5,2 | 3,9 | 13,3 | 5,6 | 3,0 | 0,0 | 0,0 | 0 | 0 | 12,9 |
| 3435-3445 | 49,7 | 3,1 | 2,2 | 15,6 | 3,3 | 13,4 | 2,6 | 0,0 | 0 | 4,8 | 5,3 |
| 3480-3490 | 30,1 | 5,6 | 2,2 | 21,2 | 2,7 | 5,9 | 5,0 | 0,0 | 0 | 7,9 | 19,4 |
| 3490-3500 | 31,2 | 5,7 | 3,0 | 13,6 | 6,5 | 4,2 | 3,2 | 0,0 | 0 | 0 | 32,6 |
| 3500-3510 | 21,6 | 0,0 | 2,3 | 28,5 | 5,1 | 6,2 | 0,0 | 0,0 | 0 | 0 | 36,3 |
| 3515-3525 | 53,8 | 3,6 | 2,2 | 11,9 | 10,9 | 6,7 | 0,0 | 0,0 | 0 | 0 | 10,9 |
| 3585-3590 | 51,4 | 3,0 | 3,7 | 18,9 | 6,5 | 4,6 | 3,7 | 0,0 | 0 | 4,7 | 3,5 |
| 3590-3603 | 27,8 | 7,0 | 11,4 | 22,8 | 2,9 | 5,3 | 4,5 | 0,0 | 0 | 5,5 | 12,8 |

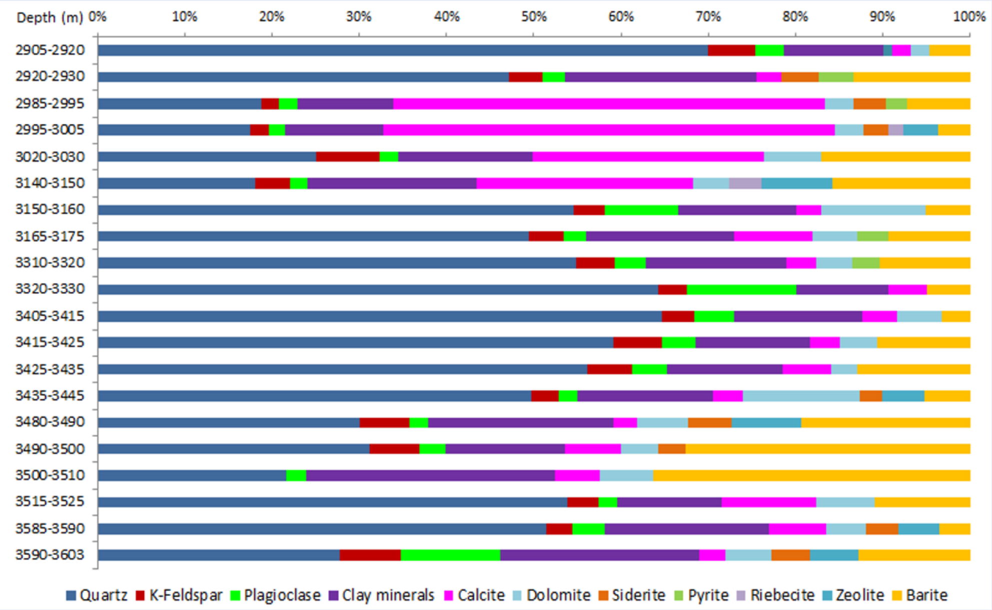


**Figure 8**: The percentage distribution of the mineral composition of the Upper Miocene deposits with the progress of the A-1X drilling depth

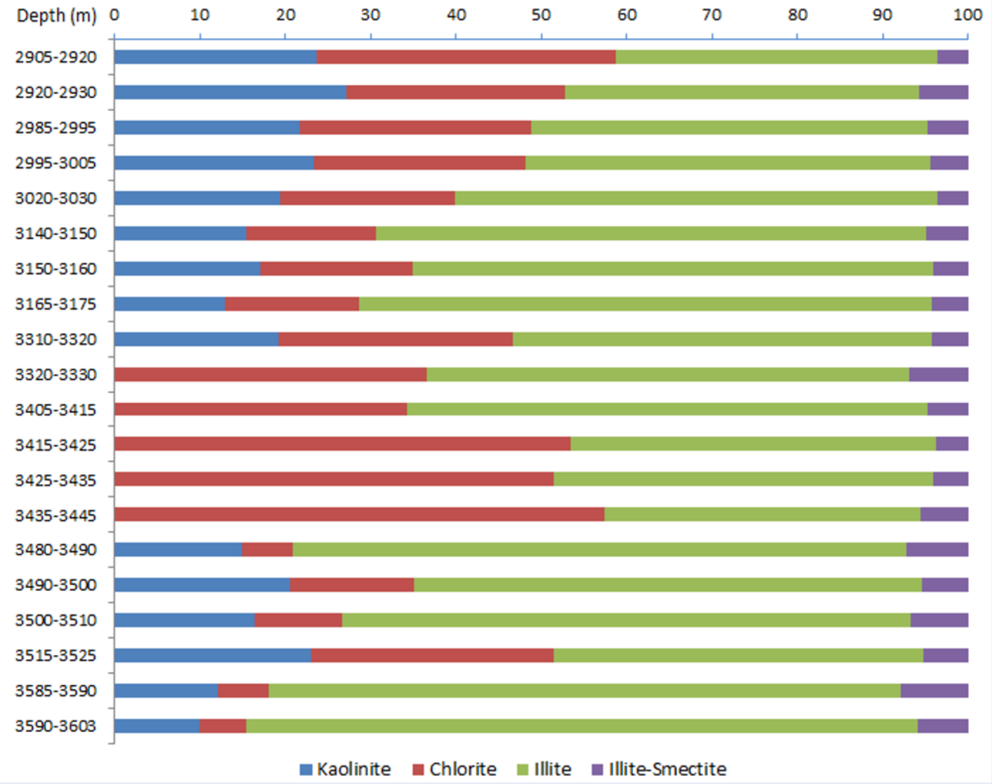


**Figure 9**: The percentage distribution of the clay mineral composition of the Upper Miocene deposits with the progress of the A-1X drilling depth

Table 5: Clay minerals of Upper Miocene sediments

| Depth (m) | Kaolinite | Chlorite | Illite | Illite-Smectite |
|---|---|---|---|---|
| 2905-2920 | 23,7 | 35,0 | 37,7 | 3,6 |
| 2920-2930 | 27,1 | 25,7 | 41,5 | 5,7 |
| 2985-2995 | 21,7 | 27,1 | 46,5 | 4,7 |
| 2995-3005 | 23,4 | 24,8 | 47,4 | 4,4 |
| 3020-3030 | 19,4 | 20,5 | 56,5 | 3,6 |
| 3140-3150 | 15,4 | 15,3 | 64,5 | 4,8 |
| 3150-3160 | 17,1 | 17,8 | 61,0 | 4,1 |
| 3165-3175 | 12,9 | 15,8 | 67,0 | 4,3 |
| 3310-3320 | 19,3 | 27,3 | 49,2 | 4,2 |
| 3320-3330 | - | 36,6 | 56,6 | 6,8 |
| 3405-3415 | - | 34,3 | 61,0 | 4,7 |
| 3415-3425 | - | 53,5 | 42,8 | 3,7 |
| 3425-3435 | - | 51,4 | 44,5 | 4,1 |
| 3435-3445 | - | 57,5 | 36,9 | 5,6 |
| 3480-3490 | 14,9 | 6,0 | 71,9 | 7,2 |
| 3490-3500 | 20,6 | 14,5 | 59,5 | 5,4 |
| 3500-3510 | 16,5 | 10,1 | 66,7 | 6,7 |
| 3515-3525 | 23,1 | 28,4 | 43,3 | 5,2 |
| 3585-3590 | 12,2 | 5,8 | 74,1 | 7,9 |
| 3590-3603 | 10,0 | 5,5 | 78,6 | 5,9 |

m, probably indicating that an amount of gas could have been generated from these source rocks and/or from deeper source rocks.

The hydrocarbons have been generated in the Upper Miocene source rock (~6.5 Ma) and Pliocene (~3.5 Ma) and probably continuing in shallow Pleistocene shale (~1.8 Ma) (Figure 10A). This implies that gas has been generated from these source rocks and accumulated in very thin sand reservoirs or their self-source reservoirs with a limited amount of gas. The wet gas/condensate has mainly been generated in the Upper Miocene source rocks that are related to the high rate of sedimentation, high heat flow or shale diapirs [17] rather than basin evolution during Pliocene and Upper Miocene with a corresponding bottom hole temperature of 163$^{o}$C and the present-day maximum vitrinite reflectance of 1.30 %. The BHT is calculated from extrapolated static and geothermal gradient of 4$^{o}$C/100m and sea bed temperature is assumed to be 20.10$^{o}$C (Figure 13A and Figure 13B).

The amount of hydrocarbon generation and expulsion was evaluated based on the transformation ratio (TR) and kerogen type. The TR changes with maturity and used for predicting the timing of petroleum generation and expulsion [8]. Hydrocarbon generation occurred in three stages, i.e. the first stage in Pliocene with gas generation and without expulsion with TR approx. 8.5% (1,921-2,651 m), the second stage in Upper Miocene with wet gas/condensate generation phase and TR approx. 11-69.42 % (2,651-3,160 m), the third stage of dry gas phase in Upper Miocene with TR approx. 0.45-1.42 % (3,160-3,602 m) (Figure 11A, Figure 11B and Figure 12A, Figure 12B).

## Petroleum system modeling

Upper Miocene and Pliocene formations are predominantly with thick shales interbedded with some very thin sands in the Upper Miocene. The generation, migration and accumulation of hydrocarbons began during Upper Miocene and Pliocene about 5.5 Ma and continuing till the present day. Pliocene shales act as self-sources and seal, probably generating some amounts of biogenic gas. Therefore, it is thought that

**Table 6: Input parameters used for 1D Petroleum system modeling**

| Formation | Pliocene | Upper Miocene |
|---|---|---|
| Age (Ma) | 5.6-2.6 | 11.6-5.6 |
| Depth (m) | 50-2,651 | 2,651-3,603 |
| Thickness of shale (m) | 1,210 | 762 |
| Thickness of erosion (m)<br>Depth of erosion (m) | 12<br>2,651 | |
| Boundary conditions: | | |
| PWD (m) | 50 | 20 |
| SWIT (oC) | 20.2 | 20.9 |
| HF (mW/m2) | 67 | 75 |

*HF= thermal conductivity of rock * geothermal gradient*
*Parameters of McKenzie model: ß mantle=3 and ß crust=1.9; $T_{swi}$ = 25.52 $^{o}C$; $T_b$= 1333$^{o}C$; hc=30 km; hm=95 km; $t_s$=23 Ma*

two types of gas reservoir existing in this well, including gas from self-sourced reservoir (unconventional) and gas from sand reservoir (conventional). Gas has been generated from both Pliocene and Upper Miocene shale reservoirs (2,700-3,345 m) and sand reservoirs (3,345-3,602 m) that Pliocene shales possibly play roles as a cap rock and shale reservoir for shale gas.

### Volumetric calculations

The results are considered and estimated only for effective source rocks. The present-day transformation ratios vary between 8-89 % in Pliocene and 0.01-0.75 % in Upper Miocene (Figure 11A) with generation mass approx. 17.88 Mtons, mainly for gas. The expulsion of gas mainly occurred in shallow depth of Pliocene and a part of Upper Miocene formations (2,500-3,000 m) with approx. 4.3 Mtons/km$^2$ (Figure 11A, B and Figure 12A, B). The generated hydrocarbons were accumulated in the source rocks that adsorbed by the organic matters and maybe lost on the migration pathways. The migration may occur in vertical or horizontal direction based on the rock properties, i.e., fractures in shales, mineral compositions. The remaining of kerogen is estimated approx. 62.81 Mtons and gas initial in place approx. 1.49 (Tcf) (Table 7).

## CONCLUSIONS

Based on interpretation of all data of well A-1X, the main concluding remarks are drawn as follows:

**Source rock properties**

The Pliocene and Upper Miocene shales are poor to fair organic richness, mainly originating from type III kerogen, containing poor to fair hydrocarbon generation potential. The Pliocene and Upper Miocene shales are currently active and probably generating an amount of gas. Deeper shales would be more effective source rocks that can produce a significant amount of gas from sand and shale reservoirs

**Petroleum system**

Hydrocarbon generation mainly related to basin burial history rather than basin evolution during the deposition from Upper Miocene to Pliocene. The burial history model shows the oil window starts at 2,700 m in the Pliocene and spreading to a part of the Upper Miocene. The organic matters are mostly favorable for gas-prone that have reached gas generation onset in the interval 1,986-3,456 m of the Upper Miocene. Gases are probably originated from biogenic gas and thermogenic gas with high $CO_2$ contents. The mass is estimated about 17.88 Mtons, hydrocarbon expulsion starts at the Upper Miocene to Pliocene (~9-5.1 Ma) with approx. 4.3 Mtons/km$^2$. The expulsion recently started in Pleistocene (∼1.8 Ma) after both the generation of gas in the Upper Miocene and Pliocene. The remaining of kerogen is estimated approx. 62.81 Mtons and GIIP of about 1.49 (Tcf).

**Shale gas properties**

Shale gas is found in the interval 2700-3290 m and the main shale reservoir at 3000-3290 m with the thickness of shale about 345 m. The shales contain a moderate quantity of Total Organic Carbon contents, deriving from type III kerogen with a little type II kerogen. The organic matters are in mature stage and possibly generating a sufficient amount of gas. Brittle minerals are dominant in the shales, indicating a favorable condition for the fracturing.

Although the data show favorable conditions for additional shale reservoirs in this well, however, the uncertainties probably come from the high CO2 content

**Table 7: Volumetric estimations**

| Parameters | Calculations | | Remarks |
|---|---|---|---|
| | Pliocene | Upper Miocene | |
| A, km2 | 40 | 40 | Area |
| hsand, m | 10 | 22 | thickness of sand |
| hshale, m | 480 | 590 | thickness of shale |
| Vsand, km3 | 400 | 880 | volume of sand |
| Vshale, km3 | 19.200 | 23.600 | volume of shale |
| $\varphi$, % | 0,05 | 0,05 | porosity |
| w, % | 0,60 | 0,60 | water saturation |
| g | 0,0283 | 0,0283 | B factor of gas |
| Free GIIP, Tcf | 0,58 | 0,71 | free gas initial in place |
| TOC, wt.% | 0,17 | 0,54 | Total organic carbon |
| Ro, % | 0,56 | 0,66 | vitrinite reflectance |
| Tres, oC | 90 | 168,3 | reservoir temperature |
| res, psi | 4.136 | 6.600 | reservoir pressure |
| VL, km3 | 2.511 | 3.732 | Langmuir volume |
| L, psi | 734 | 771 | Langmuir pressure |
| Vads, Tcf | 0,08 | 0,12 | volume of adsorbed gas |
| Total GIIP, Tcf | 0,66 | 0,83 | total gas initial in place |

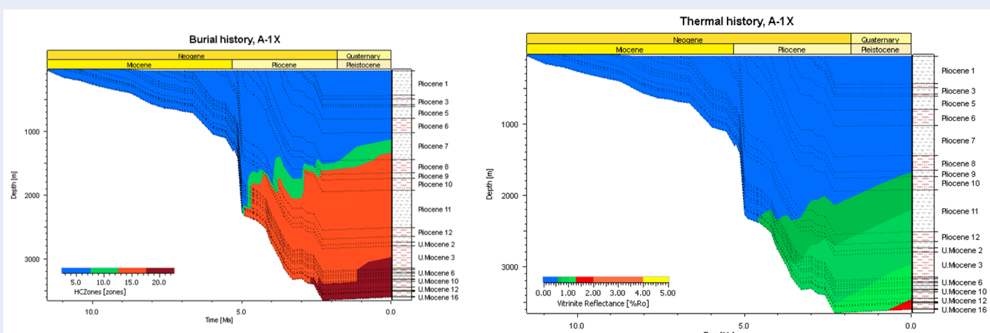


**Figure 10**: Burial history model (A); Thermal history model (B)

in this well and hydraulic fracturing technique need to be considered for further studies.

## CONFLICT OF INTEREST

On be half of the authors. I would like to declare that:

This manuscript is an original version and has not been published before and is not currently being considered for publication anywhere;

## AUTHOR CONTRIBUTIONS

I would like to confirm that the manuscript has been read and approved by all named authors and thus there are no any others who satisfied the criteria for authorship but not listed here. Moreover, order of the authors listed in the paper has been approved by all of us with our contribution to the contents of manuscript as follows:

- Corresponding author: Vo Thi Hai Quan

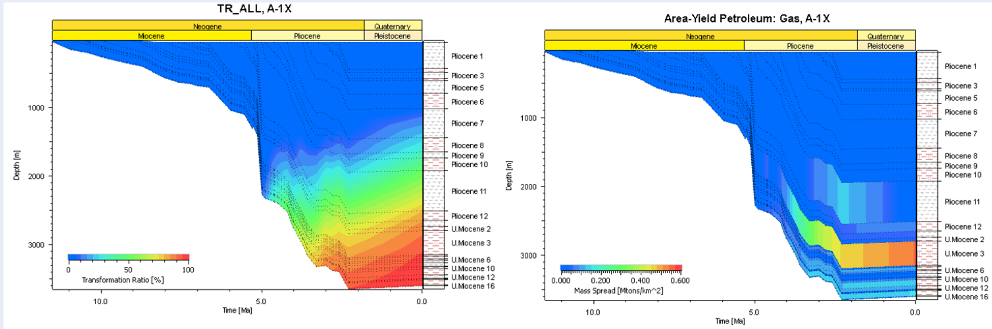


**Figure 11**: Transformation ratio (A); Area-yield gas (B)

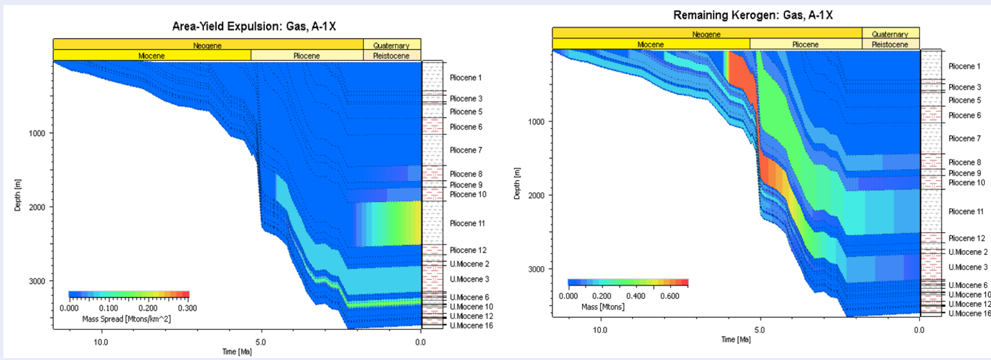


**Figure 12**: Area-yield expulsion (A); Remaining kerogen for generating gas (B)

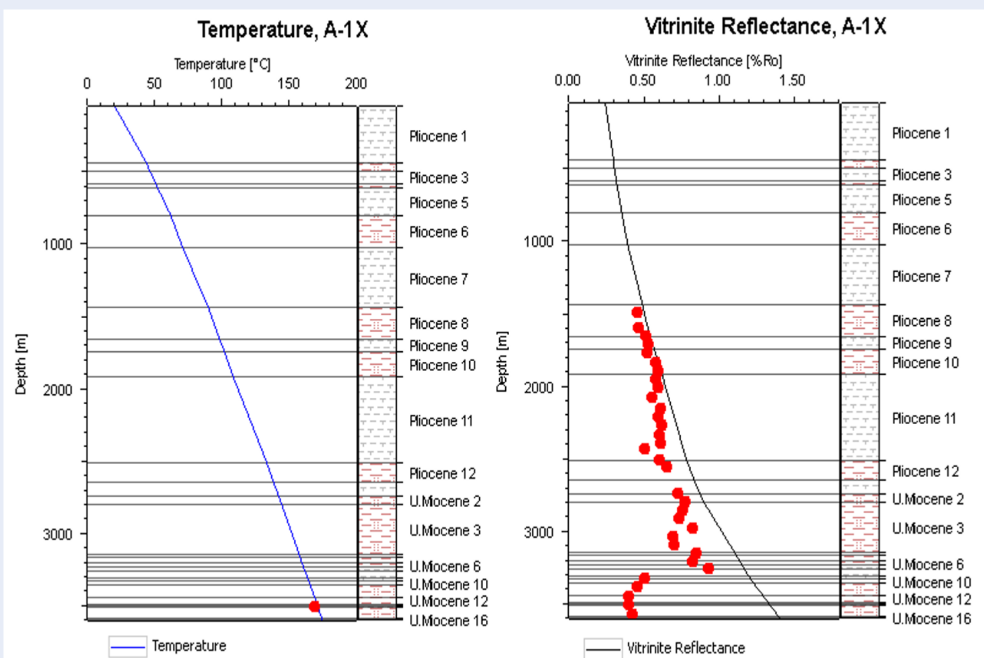


**Figure 13**: Calibration between measured and calculated temperature (A) and Ro (B)

Doing all the contents of manuscript;
- Author (1, 2): Pham Huy Giao

Revising all the contents of manuscript, especially in the main parts such as Abstract, results and Discussion, and Conclusions
- Author (3): Anna Wysocka,

Revising all the contents of manuscript, especially in the main parts such as Geological setting, Mineral compositions and Conclusions

As a corresponding author, I understand that I am responsible for communicating with the other authors to revise all the comments from the reviewers and Editorial Board.

## REFERENCES

1. PVN. The petroleum geology and resources of Vietnam. 2nd ed. Hanoi, Vietnam: Science and Technology Publication; 2019;.
2. Clip PD, Sun Z. The sedimentation and tectonic evolution of the Yingggehai-Song Hong basin and the southern Hainan margin, South China sea: Implications for Tibetan uplift and monsoon intensification. J Geophys Res. 2006;111;Available from: https://doi.org/10.1029/2005JB004048.
3. Sun Z, Zhou D, Zhong Z, Zeng Z, Wu S. Experimental evidence for the dynamics of the formation of the Yinggehai basin, NW South China Sea. Tectonophysics. 2003;372:41-58;Available from: https://doi.org/10.1016/S0040-1951(03)00230-0.
4. Kevin MKR, Martin N, Daniel P, Kenneth P, Artur S. Basic petroleum geochemistry for source rock evaluation. Oilfield Rev. 2011;23(2):32-43;.
5. Peters KE, Cassa MR. Applied Source-Rock Geochemistry. In: Magoon LB, Dow WG, editors. The Petroleum System. From Source to Trap. Tulsa: American Association of Petroleum Geologists; 1994. p. 93-120;Available from: https://doi.org/10.1306/M60585C5.
6. Peters KE. Guideline for evaluating petroleum source rocks using programmed pyrolysis. AAPG Bull. 1986;70(3):318-29;Available from: https://doi.org/10.1306/94885688-1704-11D7-8645000102C1865D.
7. Bruce M, Andrew I. Bruker D8 Advance Powder XRD instrument manual and standard operating procedure [Document]. University of Kansas; 2006;.
8. Dembicki H Jr. Practical petroleum geochemistry for exploration and production [Book]. Elsevier; 2017;.
9. Wygrala BP. Integrated study of an oil field in the southern Po Basin, Northern Italy [PhD thesis]. University of Cologne; 1989. 217 p;.
10. McKenzie D. Some remarks on the development of sedimentary basins. Earth Planet Sci Lett. 1978;40(1):25-32;Available from: https://doi.org/10.1016/0012-821X(78)90071-7.
11. Sweeney JJ, Burnham AK. Evaluation of a simple model of vitrinite reflectance based on chemical kinetics. AAPG Bull. 1990;74(10):1559-70;Available from: https://doi.org/10.1306/0C9B251F-1710-11D7-8645000102C1865D.
12. Burnham A, Sweeney J. A chemical kinetic model of vitrinite maturation and reflectance. Geochim Cosmochim Acta. 1989;53:2649-57;Available from: https://doi.org/10.1016/0016-7037(89)90136-1.
13. Pepper AS, Corvi PJ. Simple kinetic models of petroleum formation. Part I: Oil and gas generation from kerogen. Mar Pet Geol. 1995;12(3):291-319;Available from: https://doi.org/10.1016/0264-8172(95)98381-E.
14. Robert JC, Steve C. Thermal Conductivity of Organic Shales and Coals - How Their Presence and Persistence Affect Thermal Maturity. AAPG Annual Convention and Exhibition; 2015. Article #41672;.
15. Zhang L. Fractured wells in rectangular gas reservoirs with SRV. Dev Pet Sci. 2019;66:191-236;Available from: https://doi.org/10.1016/B978-0-444-64315-5.00007-3.
16. Barker C. Thermal modeling of petroleum generation theory and application. Elsevier; 1996. Development in Petroleum Science, 45;.
17. Siling Z, Jinfeng Z, Junsheng L, Yajuan Y, Pibo S. Geological characteristics of mud volcanoes and diapirs in the Northern continental margin of South China Sea: Implication for the mechanisms controlling the genesis of fluid leakage structures. 2021; Article ID 5519264, 17 pages;Available from: https://doi.org/10.1155/2021/5519264.

*Tạp chí Phát triển Khoa học và Công nghệ – Engineering and Technology 2024, 6(SI7):69-85*

Open Access Full Text Article

*Bài nghiên cứu*

# Các đặc điểm Địa hóa và Thạch học khí đá phiến sét kỷ Tân sinh của trung tâm bể Sông Hồng, Việt Nam

**Võ Thị Hải Quan[1,*], Phạm Huy Giao[1,2], Anna Wysocka[3]**

[1]Phòng Địa hóa, Viện Dầu Khí Việt Nam

[2]Trường Đại học Dầu khí; Chuyên gia, Viện Dầu khí Việt Nam

[3]Khoa Địa chất, Trường đại học Warsaw, Ba Lan

**Liên hệ**

**Võ Thị Hải Quan**, Phòng Địa hóa, Viện Dầu Khí Việt Nam

Email: quanvth@vpi.pvn.vn

**TÓM TẮT**

Bể Sông Hồng nhìn chung được xem là có ba phân vùng địa chất khác nhau gồm vùng phía Bắc, trung tâm và phía Nam, trong đó khu vực trung tâm bể được thăm dò dầu khí ít hơn so với hai khu vực còn lại. Những phát hiện khí gần đây ở khu vực trung tâm bể Sông Hồng đã thu hút nhiều sự quan tâm của các nhà thăm dò dầu khí trong và ngoài nước với những nghiên cứu và đánh giá thêm về tiềm năng sinh hydrocarbon của đá mẹ khu vực này. Trong phạm vi nghiên cứu này, các mẫu sét kết tuổi Miocene và Pliocene của giếng khoan A-1X ở trung tâm bể Sông Hồng được phân tích đánh giá các đặc điểm về Địa hóa đá mẹ và tiềm năng sinh hydrocarbon dựa trên các kết quả phân tích Địa hóa, nhiễu xạ tia X, tài liệu giếng khoan và mô hình hệ thống dầu khí. Kết quả cho thấy tổng hàm lượng carbon hữu cơ (TOC) trong hầu hết các mẫu sét Pliocene là nghèo (0,15-0,21%) và trong các mẫu sét Miocene trên là trung bình (0,19-0,79%) cho thấy các đá mẹ này có tiềm năng sinh hydrocarbon từ nghèo đến trung bình. Vật chất hữu cơ chủ yếu có nguồn gốc từ thực vật bậc cao của kerogen loại III và có trộn lẫn một ít kerogen loại II từ tảo. Kết quả đo độ phản xạ vitrinite cho các mẫu sét kết Pliocene (0,45-0,65%) và một phần của Miocene trên (0,72-0,93%) cho thấy các mẫu sét này có mức độ trưởng thành nhiệt tương đồng với nhiệt độ đo được ở đáy giếng khoan là 163$^{o}$C. Kết quả từ các mô hình lịch sử chôn vùi trầm tích và địa nhiệt cho thấy tốc độ trầm tích hóa nhanh đã ảnh hưởng tới việc gia tăng nhiệt độ trong các mẫu sét kết Pliocene và Miocene trên nên vật chất hữu cơ của các đá mẹ này đang trong giai đoạn từ trưởng thành đến cửa sổ tạo dầu. Các mô hình cho thấy hydrocarbon được sinh ra trong giai đoạn trưởng thành sớm từ đá mẹ Pliocene với độ phản xạ vitrinite là Ro=0,60% và trong pha tạo dầu chính từ đá mẹ Miocene trên với vitrinite là Ro=0,80%. Các kết quả trong nghiên cứu này cho thấy sét kết Pliocene và Miocene trên có thể được xem là có tiềm năng sinh khí từ vật chất hữu cơ có nguồn gốc sinh học và địa nhiệt. Tổng lượng khí sinh ra được ước lượng khoảng 17,88 triệu tấn, lượng khí di thoát khoảng 4,3 triệu tấn/km$^2$ và lượng kerogen còn lại khoảng 62,81 triệu tấn, khí tại chỗ khoảng 1,49 tỷ khối feet. Bên cạnh đó đá phiến sét ở sâu hơn được xem là những đá mẹ hiệu quả hơn cho những triển vọng khí mới.

**Từ khoá:** Khí đá phiến sét, Đá mẹ, Phản xạ vitrinite, Nhiễu xạ tia X, Hệ thống dầu khí, Bể Sông Hồng

**Lịch sử**
- Ngày nhận: 29-9-2023
- Ngày chấp nhận: 17-5-2024
- Ngày đăng: 31-12-2024

**DOI : 10.32508/stdjet.v6iSI7.1238**

Check for updates

**Bản quyền**

© ĐHQG Tp.HCM. Đây là bài báo công bố mở được phát hành theo các điều khoản của the Creative Commons Attribution 4.0 International license.

VNUHCM PRESS

**Trích dẫn bài báo này:** Quan V T H, Giao P H, Wysocka A. **Các đặc điểm Địa hóa và Thạch học khí đá phiến sét kỷ Tân sinh của trung tâm bể Sông Hồng, Việt Nam**. *Sci. Tech. Dev. J. - Eng. Tech.* 2024; 6(SI7):69-85.